TABLE 1 Comparison of Bandpass Filters with Wideband Spurious Suppression

| Ref. | Center Frequency (GHz) | Dielectric Constant ($\varepsilon_r$) | 3 dB FBW | Insertion Loss (dB) | Return Loss (dB) | External Quality Factor ($Q_E$) | Spurious Suppression ($nf_0$) | Rejection Level (dB) | Size ($\lambda_g \times \lambda_g$) |
|---|---|---|---|---|---|---|---|---|---|
| [2] | 2.3 | 2.5 | 6.52% | <0.67 | <−22 | 15.3 | $4.35f_0$ | >23 | 0.535 $\lambda_g$ × 0.357 $\lambda_g$ |
| [3] | 2.44 | 2.2 | 3.3% | <1.93 | <−20 | 24.4 | $6.55f_0$ | >20 | 0.206 $\lambda_g$ × 0.152 $\lambda_g$ |
| [4] | 1.5 | 2.2 | 10% | <3.03 | <−15 | 11.47 | $8.2f_0$ | >30 | 0.768 $\lambda_g$ × 0.137 $\lambda_g$ |
| [5] | 1.51 | 3.38 | 4.5% | <4.05 | <−17 | 21.1 | $8.2f_0$ | >30 | 0.323 $\lambda_g$ × 0.224 $\lambda_g$ |
| This work | **2.25** | **2.2** | **17.7%** | **<1.73** | **<−21** | **5.65** | **$9.1f_0$** | **>30.5** | **0.553 $\lambda_g$ × 0.242 $\lambda_g$** |

which has the merit of particularly narrow band selectivity. Only the fundamental resonance is highly selected to the feeding I/O ports, which can be demonstrated by the typical stopband simulated electric current density (i.e., 13.3 GHz) of the structure shown in Figure 5. It can be seen that the closed electronic and magnetic coupling paths in the tight coupled DGS TSCFs and microstrip T-stubs lead to low radiation and free spurious. Besides, from the transmission and reflection characteristics of the structure depicted in Figure 4, it demonstrates a low radiation stopband with good spurious suppression in the wide frequency range from the first spurious $P_{p2}$ up to 20 GHz. Thus, the wide stopband responses are from the intrinsic characteristics of the proposed structure. Based on the investigation above, it can be concluded that the proposed scheme has the following two functions: (1) high selectivity on the fundamental frequency; (2) high rejection on high-order modes or spurious. In addition, it is found that an optimized stopband frequency responses can be obtained, when the ratios of the DGS dimensions (i.e., $S_1$: $W_A$: $S_2$) and the T-stub (i.e., $W_2$ to $L_2/2$) are chosen at 3:1:1 and 3:4, respectively.

## 3. EXPERIMENTAL RESULTS

Based on the procedures above, a bandpass filter with wide stopband is implemented and fabricated. The proposed filter is designed with a center frequency of $f_0$ = 2.2 GHz, 3 dB fractional bandwidth (FBW) of 17.5%, $M_{12} = M_{23} = 0.135$, and $Q_E = 5.70$. The dimensions of the filter are same as the Case (b) in Figure 4, and the total size of the filter is about 55.0 mm by 24.1 mm. The measurement is performed using the Agilent 5230A Network Analyzer from 10 to 20 GHz. As depicted in Figure 6, the measured results show that the proposed filter has a center frequency $f_0$ of 2.25 GHz, 3 dB FBW of 17.7%, maximum insertion loss of 1.73 dB, and typical return loss about 21 dB. Specifically, the wide stopband of the bandpass filter is extended to 20 GHz (about 9.1 $f_0$) with a satisfactory rejection level greater than 30.5 dB.

Table 1 compares the fabricated filter in this letter with some bandpass filters with wide stopband recently reported [2–5]. It is notable that our filter with a relatively wide passband (i.e., 400 MHz) and the strong enough stopband performance is competitive.

## 4. CONCLUSIONS

In this letter, a bandpass filter with wide stopband of 9.1 $f_0$ is proposed using the broadside-coupled microstrip T-stub/DGS cells. Finely adjusted resonance and wideband spurious suppression are used by the cells with an interdigital coupled scheme. With good passband and stopband performances, the proposed filter is attractive for the practical applications.

## REFERENCES


1. J.S. Hong and M.J. Lancaster, Microstrip filters for RF/microwave applications, Wiley, New York, 2001.
2. C.-S. Kim, D.-H. Kim, I.-S. Song, K.M.K.H. Leong, T. Itoh, and D. Ahn, A design of a ring bandpass filters with wide rejection band using DGS and spur-line coupling structures, in IEEE MTT-S International Microwave Symposium Digest, Anaheim, CA, May 2005.
3. X. Luo and J.-G. Ma, Compact slot-line bandpass filter using backside microstrip open-stubs and air-bridge structure for spurious Suppression, in Proceedings of the Asia-Pacific Microwave Conference, Dec. 2009.
4. J.-T. Kuo and E. Shih, Microstrip stepped impedance resonator bandpass filter with an extended optimal rejection bandwidth, IEEE Trans Microwave Theory Tech 51 (2003), 1554–1559.
5. C.-F. Chen, T.-Y. Huang, and R.-B. Wu, Design of microstrip bandpass filters with multiorder spurious-mode suppression, IEEE Trans Microwave Theory Tech 53 (2005), 3788–3793.
6. Zeland Software, IE3D 12.32, Zeland Software, California, 2007.
7. D. Ahn, J.S. Park, C.S. Kim, Y. Qian, and T. Itoh, A design of the lowpass filter using the novel microstrip defected ground structure, IEEE Trans Microwave Theory Tech 49 (2001), 86–93.
8. S. Amari, Direct synthsis of folded symmetric resonator filters with source-loading coupling, IEEE Microwave Wirel Compon Lett 11 (2001), 264–266.




# ANOMALOUS FORERUNNERS IN WAVE PROPAGATION INTERPRETED BY A TYPICAL DIFFRACTION INTEGRAL


**A. Ranfagni,[1] I. Cacciari,[1] R. Ruggeri,[2] A. Agresti,[3] R. Mignani,[4] A. M. Ricci,[5] and A. Petrucci[4]**

[1] Istituto di Fisica Applicata "Nello Carrara" del Consiglio Nazionale delle Ricerche, via Madonna del Piano 10, 50019 Sesto Fiorentino, Firenze, Italy

[2] Istituto dei Sistemi Complessi del Consiglio Nazionale delle Ricerche, Sezione di Firenze, via Madonna del Piano 10, 50019 Sesto Fiorentino, Firenze, Italy; Corresponding author: rocco.ruggeri@isc.cnr.it

[3] Dipartimento di Fisica dell'Universitá di Firenze, via G. Sansone 1, 50019 Sesto Fiorentino, Firenze, Italy

[4] Dipartimento di Fisica "Edoardo Amaldi" Universita' degli Studi di Roma "Roma Tre", via della Vasca Navale 84, 00146 Roma, Italy

[5] Istituto per le Telecomunicazioni e l'Elettronica della Marina Militare "Giancarlo Vallauri" (Mariteleradar), Viale Italia 72, 57100 Livorno, Italy


*Received 11 November 2010*


**ABSTRACT:** *By using radar techniques over distances of 16 and 80 m, microwave propagation experiments revealed the presence of anomalous forerunners situated in advanced positions with respect to the main (luminal) peak. These results can be interpreted by a typical diffraction integral, which accounts for the existence of (fast) complex waves, which are usually considered only in the near-field region, but are still surviving beyond this limit.* © 2011 Wiley Periodicals, Inc. Microwave Opt Technol Lett 53:1789–1793, 2011; View this article online at wileyonlinelibrary.com. DOI 10.1002/mop.26133


**Key words:** *asymptotic expansions; diffractions; electromagnetics*

## 1. INTRODUCTION

The celebrated works by Sommerfeld and Brillouin on wave propagation [1] denied the possibility of forerunners, advanced with respect to the main signal if it is propagating at light velocity in vacuum. This result holds for dispersive media in which the various velocities (of phase, group, and signal) are different. Superluminal behaviors were admissible for the phase and group velocities but not for the signal. Superluminal propagations have been demonstrated in several cases (Among the several contributions, we mention only a few that are representative of different cases [2–5]), and there is now no question that this effect has been observed. Thus, the controversial issues revolve around the nature of signaling. This has led to challenges at both theoretical and experimental levels [6–8 (G. Nimtz, Nature (London) 429 (06 May 2004) Brief Commmun.),9, 10]. Without entering in the disputable (let us say, almost inexstricable) definition of signal, in this article, we recall and discuss the results that show the presence of forerunners in microwave propagations even beyond the near-field limit and which overcome the luminal barrier. Such results are relative, for the way in which the experiments were carried out, with the group velocity, given the presence of moderate dispersion. This is evidently a crucial point since, even if the possibility of a superluminal behavior is normally admissible for the group velocity, it is usually considered impossible for the signal one. Thus, the observed superluminality could be referred to an apparent effect as due to properties of relativistic field equations, as in [11] for dispersive situations, or to geometric effects due to the angle between the propagation axis and the one of observation [12], for the cases in absence of dispersion. Evidence of superluminal behaviors has already been obtained both in processes of optical and microwave tunneling (where dispersion is present and important) over distances of the order of the wavelength [Among the several contributions, we mention only a few that are representative of different cases. a), b)], and in processes of propagation (with presumed negligible dispersion) in which the effects have been evidenced up to distances of the order of tens of wavelengths, but still inside the so-called near-field limit. By increasing the distance, the effect disappeared due to a prevalence of the normal (luminal) wave over the anomalous (superluminal) one [Among the several contributions, we mention only a few that are representative of different cases. c), d)]. We remark that independently of the proposed interpretations—several other ones have been suggested of different kind [13, 14], even of exotic type [15]—the most interesting aspect of this phenomenology is the experimental observation and the relative results. In the course of this work, we limit ourselves to recall some recent results, giving a plausible interpretation of them, renouncing to give a conclusion on the meaning of signaling.

Recently, the use of sophisticated measurement techniques (i.e., radar systems) has made it possible to overcome the near-field limit, since the systems used allowed for the detection of forerunners (that is placed in advance with respect to the normal wave) even when their intensity was 30–40 dB lower than the main luminal echo [9]. Even if the generating mechanism of these "anomalous waves" is mainly inherent in situations of near-field, we can demonstrate the possibility of evidencing them up to distances of several hundreds of wavelengths.

Before recalling and discussing the abovementioned results, we premise a detailed analysis of the mechanism, which generates these anomalous waves (complex waves) that is typical of diffraction phenomena. This implies an evaluation of integrals, which, in general, cannot be evaluated in closed form, but rather by means of an asymptotic expansion that holds for large values of a parameter. There are various methods for obtaining this asymptotic expansion. We will mainly follow the method reported in the classical work by Felsen and Marcuvitz [16], even if several other contributions are available in the literature [17–19]. A problem arose just about an evaluation of the strong intensity of the main peak due to the normal (luminal) wave. The adoption of a suitable fitting parameter allowed for the obtaining of a good agreement with the experimental results.

## 2. DIFFRACTION INTEGRALS

The field amplitude emitted by a rectangular aperture (in our case, the mouth of the horn launcher) can be expressed by a diffraction integral, to be computed along the steepest descent path (SDP). This is given by

$$I(\Omega) = \int_{\mathrm{SDP}} f(z)\exp[\Omega q(z)]dz \tag{1}$$

where $\Omega = 2\pi\rho/\lambda$, $f(z) = a(z-\beta)^{-1}$ with $a$ a numerical coefficient, $\beta = \beta_r + i\beta_i \equiv z_0$ is the angular coordinate of a pole singularity in the complex plane of the $z = x + iy$ angle, which can be: (i) far, (ii) near, or (iii) coincident with the saddle point of $q(z) = i\cos(z-\alpha)$ at $z_S = \alpha$, with $\alpha$ and $\rho$ being the polar coordinates of the observation point and $\lambda$ the wavelength. Integral (1) will be evaluated within the limit of high values of $\Omega$, by considering only the leading terms of the order of $\Omega^{-1/2}$. As the saddle point at $z_S$ is of the first order, a change of variables from $z$ to $s$ is given by $q(z) = q(z_S) - s^2$. After substitutions, Eq. (1) becomes

$$I(\Omega) = e^{\Omega q(zS)}\int_{-\infty}^{+\infty} G(s)e^{-\Omega s^2}ds, \tag{2}$$

with $G(s) = f(z)dz/ds = a/(s-b) + T(s)$, and $b = \sqrt{q(z_S) - q(z_0)}$. Thus, $I(\Omega)$ can be expressed as the sum of two contributions, namely

$$I(\Omega) = e^{\Omega q(zS)}\left[\int_{-\infty}^{+\infty}\frac{a}{s-b}e^{-\Omega s^2}ds + \int_{-\infty}^{+\infty} T(s)e^{-\Omega s^2}ds\right]. \tag{3}$$

where for $T(s) = T(0) + T'(0)s + \ldots$, according to the saddle-point method, only the first term $T(0)$ will be considered given by $T(0) = hf(z_s) + a/b$, with $h = [-2/q''(z_s)]^{1/2}$.

In Eq. (3), the first term represents the contribution as being due to the presence of the pole singularity at $s = b$, whereas the second one can be evaluated according to the saddle-point approximation. The result of $I(\Omega)$ depends critically on the relative position of the pole singularity, with respect to the saddle point position; accordingly, we are faced with different situations. Clearly, if the pole is sufficiently far from the saddle point, case (i), the first term in (3) becomes negligible, $T(s) \to G(s)$, and $I(\Omega)$ is given by the usual saddle-point expression. In general, the first term in (3) has to be considered, case (ii), and the resulting expression for $I(\Omega)$ is found to be [16]

$$I(\Omega) \simeq e^{\Omega q(zS)}\left[\pm i2a\sqrt{\pi}e^{-\Omega b^2}Q(\mp ib\sqrt{\Omega}) + \sqrt{\frac{\pi}{\Omega}}T(0)\right], \quad \mathrm{Im}\, b \gtrless 0 \tag{4}$$

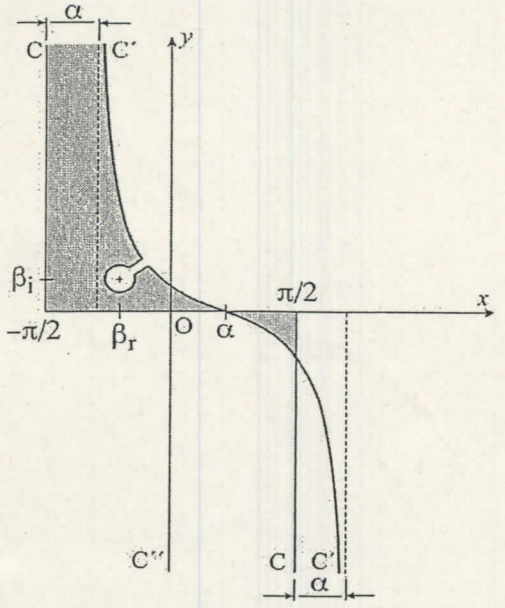


**Figure 1** The original integration path $C$: $iy$, $-\pi;/2$, $\pi;/2$, $-iy$, is deformed in the steepest descent path $C'$, taking into account pole singularities. If these are situated into the shaded areas, the corresponding complex waves have velocity greater than $c$. In our considered cases, the angle of observation is $\alpha = 0$. For Zenneck-type waves, the pole singularity is situated in the shaded area on the right, and is not crossed by the deformation of the original integration path which, in this case, reduces to $C - C''$: $iy$, $-\pi;/2$, 0, $-iy$. coincident in the original integration path as well as in the SDP, the first integral in Eq. (3) diverges and $I(\Omega) \to \infty$. A third conclusion can be drawn for the case in which the pole coordinate is coincident with the saddle point only in the SDP, but not in the original integration path. In the latter case, the divergence does not take place and the result can be still obtained with Eq. (4), with $b = 0$ [Therefore, if the wave with direction $\alpha = 0$ could be identified with a pole singularity, in accordance with the unpublished data (G. Toraldo di Francia, Metodi Matematici della Fisica, University of Florence, 1965), this can give rise to a divergency in $I(\Omega)$. In our cases, however, we never realize this situation]

where $Q(y) = \int_{-\infty}^{} e^{-x^2} dx$ is the error-function complement. We note that, when Im$b$ changes sign, the discontinuity in (4) is $2\pi i a \exp\{\Omega[q(z_S) - b^2]\} \equiv 2\pi i \operatorname{res}[f(z \to \beta)]$, as $Q(y) + Q(-y) = \sqrt{\pi}$. This residue must be added to Eq. (4) in the case that Im$b < 0$ and if the pole singularity has been crossed in deforming the integration path from the original one to the SDP, see Figure 1. In this way, $I(\Omega)$ is a continuous function of $b$. In the case that the singularity is situated on the SDP, Im$b = 0$, $Q(0) = \frac{1}{2}\sqrt{\pi}$, and the first term in (4) is exactly equal to $\pi i \operatorname{res}[f(z \to \beta)]$.

In the case that the pole position is coincident with the saddle point ($b = 0$), case (iii), the situation is more delicate, and (apparent) controversial versions can be found in the literature [, [16–19, (G. Toraldo di Francia, Metodi Matematici della Fisica, University of Florence, 1965, unpublished)]. According to [16] (see Eq. (4a) on p. 400), only the term in $T(0)$ survives in this case in Eq. (4). According to another interpretation (G. Toraldo di Francia, Metodi Matematici della Fisica, University of Florence, 1965, unpublished), which holds only when the pole position and the saddle point are indeed coincident.

## 3. NORMAL AND ANOMALOUS (COMPLEX) WAVES

According to a phenomenological model ([20], where indeed, given the finiteness of the horizontal aperture of the launcher, the directions of the waves are considered in the horizontal plane, while in the present work are attributed to the vertical one), the field emitted by a horn antenna can be roughly described by the sum of three waves, or rays, which in the vertical plane $(\eta, \xi)$, perpendicular to horn mouth, have directions $\alpha = 0$, and $\alpha = \pm\beta_r$. The waves with directions $\pm\beta_r$ give rise to pole singularities that correspond to complex waves, with phase-path velocity given by (See Ref. 4, where in the Appendix the presence of the singularities is demonstrated, in the framework of a Fresnel optics.)

$$v_{pp} = \frac{c}{\cos(\pm\beta_r)\cosh\beta_i}, \tag{5}$$

which can be greater than the light velocity $c$, and attenuate according to

$$Att. = \exp[-k\rho \sin\beta_r \sinh(\beta_i)], \tag{6}$$

where $k = 2\pi/\lambda$. The wave with direction $\alpha = 0$, the same as the observation point, is likely due to the saddle-point (luminal) contribution. Some problems arise in explaining the strong intensity of the luminal echo observed, with respect to the weak intensity of the forerunners (superluminal), which are attributed to complex waves. According to Ref. 16, by putting $a = 1$, i.e., if $f(z)$ in (1) is simply given by $(z - \beta)^{-1}$, we have that for small values of the angular separation $\alpha - \beta$ between the pole position and the saddle point, the $T(0)$ contribution in Eq. (4) turns out to be very small [as $T(0) \to 0$, for $(\alpha - \beta) \to 0$, unless terms of higher order, see Eq. (4b) on p. 400 of Ref. 16]. This implies that the first term in (4) which accounts for the pole contributions becomes the dominant one thus in contradiction with the experimental results, see below in Table 1. Therefore, as previously mentioned, we have to introduce a fitting parameter in the mathematical model. Let us consider that, in the relation.

$$G(s) = \frac{a}{s - b} + T(s), \tag{7}$$

**TABLE 1 Down Range Values $R(\equiv\rho)$ and Down-Range Variations $\Delta R$ Relative to Forerunner Intensities $\Omega I_f$ and Main-Peak Intensities $\Omega I_0$, in Arbitrary Units**

| | | $I_f(10^{-2})$ | | | | | | |
|---|---|---|---|---|---|---|---|---|
| $R$ (m) | $-\Delta R$ (cm) | Experimental Values | Theoretical Values | $I_0$ | $\beta_r$ (°) | $\beta_i$ (°) | $a^{-1}$ | Refs. |
| 16 | 56.5 | 55 | 52.8 | $\sim 10^4$ | ~15 | ~0.23 | $\sim 3 \times 10^3$ | [22] |
| 32 | 25.6 | 25 | 26.4 | | | | | |
| 80 | 16 | 70 | 53 | $>10^3$ | 8.2 | 6.5 | $\sim 2.5 \times 10^3$ | [21] |
| 160 | 48 | 24 | 22 | | 9.2 | 6.9 | | |

The values of $\beta_r$ and $\beta_i$ angles, and $a^{-1}$ factor are indicated.

the quantity $a$ could be $\gg 1$: that is, $f(z)$ is not simply given by $(z-\beta)^{-1}$, but by a different expression in which the singularity has less importance. Clearly, in this way, $T(0) \to G(0)$, and in Eq. (4), the term in $T(0)$ can prevail over the one in $\mp ib\Omega$. This is required by the physical evidence according to which the pole contributions at $\pm\beta_r$, must be of secondary importance with respect to the saddle-point contribution at $\alpha = 0$.

## 4. ANALYSIS OF THE EXPERIMENTAL RESULTS

Here, we consider the results of two distinct experiments of microwave propagation, both of which led to comparable results [9]. In one case [21], a radar system operating in the 7.5–15 GHz frequency range, was used over a feed-target distance of 80 m, 2 m above a metallized ground plane.

In the other case [22], an analogous system was used in a "compact range" (i.e., inside an anechoic chamber) over a feed-target distance of 16 m. In this case, a converging device was interposed between feed and target, thus producing a sort of amplification of the effects (The multiplet structure of the forerunners, observed in this case, is presumably due to the converging device, consisting of two cylindrical reflectors, but assimilated to a spherical system constituted by the combination of a real and a virtual lens [20]).

In both cases, the launcher and the receiver consisted of horn antennas. The targets were metal bars positioned transversally with respect to the line of sight of the radar antennas, and 6 m long in the first case and 1.5 m long in the second. The results obtained, for down range $R(\equiv \rho)$ comprised between 16 and 160 m, are summarized in Table 1 showing the positions (down-range variation $\Delta R$) of anomalous forerunners situated in advance with respect to the main specular peak, which is assumed to be zero position in the down-range variation. Their intensities, $I_f \propto |J(\Omega)|^2$, relative to the main peak intensity $I_0$ are reported for both experimental and theoretical values. The values of $\beta_r$ and $\beta_i$, which according to (5) account for the $\Delta R$ results observed (We note that in moderately dispersive situations, like the ones in our experiments, relation (5) could be assumed to hold approximately also for the group velocity.), are also indicated, together with the estimated values for $a^{-1}$.

The results relative to the experiment of Ref. 21 have been interpreted by hypothesizing the existence of Zenneck-type waves acting in one way for $R = 80$ m and in double way for $R = 160$ m, with a negative incident angle of $-\beta_r$. In this case, as pole singularity is not captured by the deformation of the original integration-path to the SDP [20] (where indeed, given the finiteness of the horizontal aperture of the launcher, the directions of the waves are considered in the horizontal plane, while in the present work are attributed to the vertical one.), [21], the amplitude of the complex (Zenneck) wave is given simply by the first term in Eq. (4). Apart from a multiplicative constant $(\pm i\pi a)$, this quantity, can be expressed by the function

$$F(\xi) = \frac{2}{\sqrt{\pi}} e^{-2i\xi^2} Q[(1-i)\xi] \simeq \frac{e^{i\pi/4}}{\sqrt{2\pi\xi}} \tag{8}$$

where $\xi = \sqrt{\Omega}|\sin\left(\frac{\beta-\alpha}{2}\right)$, which is a real quantity if $\beta \approx \beta_r$, and the last member holds for $\xi \gtrsim 1$. More generally, $|F(\xi)|$, for complex and large $\xi$ (in our case $|\xi| \simeq 12 - 18$), is given by $(\sqrt{2\pi}|\xi|)^{-1}$. The results of intensity, $\propto |J(\Omega)|^2$, which also depend on the permittivity and conductivity of the ground plane, are reported in Table I. Once they had been properly normalized to a given value [21], to put them in the right scale, they were found to be in fairly good agreement with the experimental data. As for the amplitude of the main (luminal) peak, it was proportional to $\sqrt{\lambda/\rho} = 1.37 \times 10^{-2}$, for an average $\lambda = 3$ cm and $\rho = 160$ m (Note that, under the assumption that $a \ll 1$, the contribution due to the saddle point, $\sqrt{\pi/\Omega}T(0)\exp[\Omega(z_S)]$ in (4), becomes $\sqrt{\lambda/\rho}\exp[i(k\rho - \pi/4)]$, since $T(0)$ simply holds $\sqrt{2}$. Then, by factorizing parameter $a$ in Eq. (4), the saddle point amplitude is found to be multiplied by $a^{-1}$). Once multiplied by $a^{-1} \simeq 2.5 \times 10^3$, this value gave rise to an intensity value of the order of $10^3$, in reasonable agreement with the observed one of $I_0 > 10^3$.

Less simple was the interpretation of the data relative to the experiment of Ref. 22. There, the intensity relative to the one-way path ($R = 16$ m) was found to be about one half of the intensity relative to the double-way path ($R = 32$ m) while just the opposite seemed reasonable, as in the previous case (Interference effects between contributions of $\pm\beta_r$ directions (not considered here) could partially explain this incongruity.). Therefore, a possible agreement with the experimental data could be achieved by interchanging the attribution of the forerunners, namely the more intense ($55 \times 10^{-2}$) to the one-way path, and the other ($25 \times 10^{-2}$) to the double-way path, in accordance with a different wave-path interpretation (This anomaly in the observed values of the intensity gave rise to a different interpretation of forerunners as proposed in Ref. 22. In particular, the more intense forerunner is attributed to a complex-wave path in transmission, and the return to the ordinary (luminal) wave path. On the contrary, for the less intense forerunners, even the coming back to the receiver is due to the complex-wave path. For details of calculation see 22.). In this way, we can obtain $26.4 \times 10^{-2}$ for $\rho = 32$ m, and $52.8 \times 10^{-2}$ for $\rho = 16$ m, by assuming $a^{-1} \simeq 3 \times 10^3$. These values (see Table 1) are in very good agreement with the observed ones.

Therefore, we can conclude that the model adopted is able to give a reasonable description of the experimental results, for both the intensity and the position of the superluminal forerunners, even in relation—through the adoption of a fitting parameter—to the strong intensity of the luminal main peak. The presence of even a moderate dispersion (As can be evidenced based on [23]) assures the validity of the observed superluminality only relatively to the group velocity. The relevance of the results reported lies in the fact that such behavior has been evidenced and interpreted in situations of wave propagation over distances that overcome the conventional limit of the near field.

## REFERENCES


1. L. Brillouin, Wave propagation and group velocity, Academic Press, New York, 1960.
2. For optical tunneling see, Ph. Balcou and L. Dutriaux, Phys Rev Lett 78 (1997), 851.
3. For microwaves in wave-guides below cutoff, A. Enders and G. Nimtz, J Phys (France) I 2 (1992), 1963.
4. For microwaves in free space, A. Ranfagni, P. Fabeni, G.P. Pazzi, and D. Mugnai, Phys Rev E 48 (1993), 1453.
5. D. Mugnai, A. Ranfagni and R. Ruggeri, Phys Rev Lett 84 (2000), 4830.
6. N. Brunner, V. Scarani, M. Wagmüller, M. Legré, and N. Gising, Phys Rev Lett 93 (2004), 203902.
7. M.D. Stenner, D.J. Gauthier, and M.A. Neifeld, Nature (London) 425 (2003), 695; 429 (06 May 2004) Replay.
8. W. Heitman, G. Nimtz, Phys Lett A 196, 154 (1994).
9. A. Ranfagni, P. Fabeni, G.P. Pazzi, A.M. Ricci, P. Trinci, R. Mignani, R. Ruggeri, and F. Cardone, Phys Lett A 352 (2006), 473.
10. A. Ranfagni, G. Viliani, C. Ranfagni, R. Mignani, R. Ruggeri, and A.M. Ricci, Phys Lett A 370 (2007), 370.

11. A.D. Jackson, A. Lande, and B. Lautrup, Phys Rev A 64 (2001), 044101.
12. P. Saari and K. Reivelt, Phys Rev Lett 79 (1997), 4135.
13. F. Cardone and R. Mignani, Phys Lett A 306 (2003), 265.
14. A.A. Stahlhofen and G. Nimtz, Europhys Lett 76 (2006), 189.
15. R.A. Ashworth, Phys Essay 11 (1998), 1.
16. L. B. Felsen and N. Marcuvitz, Radiation and scattering of waves, Prentics-Hall, Englewood Cliffs, New York, 1973, Sec. 4.
17. C. Gennarelli and L. Palumbo, IEEE Trans, AP-32 (1984), 1122.
18. R.G. Rojas, ibidem, AP-35 (1987), 1489.
19. P. Vaudon and B. Jecko, Microwave Opt Technol Lett 6 (1993), 252.
20. A. Ranfagni and D. Mugnai, Phys Rev E 58 (1998), 6742.
21. A. Ranfagni, P. Fabeni, G.P. Pazzi, A.M. Ricci, R. Trinci, R. Mignani, R. Ruggeri, F. Cardone, and A. Agresti, J Appl Phys 100 (2006), 024910.
22. A. Ranfagni, A.M. Ricci, R. Ruggeri, and A. Agresti, Phys Lett A 372 (2008), 6541.
23. H.M. Barlow and A.L. Cullen, Proc Inst Electr Eng 100 (1953), 329.



# NONCONTACT HEART RATE MONITORING USING DOPPLER RADAR AND CONTINUOUS WAVELET TRANSFORM

**A. Tariq and H. Ghafouri-Shiraz**
Electronic, Electrical and Computer Engineering Department, University of Birmingham Edgbaston, Birmingham, West Midlands, UK; Corresponding author: ghafourh@bham.ac.uk

*Received 11 November 2010*

**ABSTRACT:** *An algorithm based on wavelet transform is utilized in detecting and examining the heartbeat signal obtained from a Doppler radar. Time–frequency localization properties of wavelet transform were used to examine the signal and provided detail of swift and slow changes in heart rate over very small periods resulting in better determination of the accuracy of the Doppler radar. Till 1 m, a very accurate and robust performance was observed for the Doppler radar. Even at 2-m heart rate was detectable but not with reasonable accuracy.* © 2011 Wiley Periodicals, Inc. Microwave Opt Technol Lett 53:1793–1797, 2011; View this article online at wileyonlinelibrary.com. DOI 10.1002/mop.26092

**Key words:** *continuous wavelet transforms; Doppler radar*

## 1. INTRODUCTION

Microwave Doppler radar is a promising tool for monitoring the heart and breathing rate of patients with heart-related illnesses, lung disorders, diabetes, and so forth. The fixed electrodes of an electrocardiogram (ECG) may be painful or uncomfortable for burn victims or infants. Improving the quality of care for such patients can be achieved by using noninvasive cardiopulmonary monitoring [1–5].

Noninvasive monitoring devices do not require physical wires allowing freedom of movement for patients, thus their daily routine is not affected. For long-term monitoring such as during sleep, Doppler radar presents the ideal choice for a cheap, constant, and robust system. Along with aforementioned uses, Doppler radar has been used for detecting people under rubble or on the battlefield even with armor.

A 0.25 $\mu$m silicon chip with a 2.4-GHz Doppler radar was used in Ref. 1. With a single-channel chip, an accuracy from 40 to 100% was achievable but with a quadrature (I/Q) receiver, an accuracy always greater than 80% was achieved. Obeid [2] used a tunable system by changing two particular parameters, power and frequency. The affect of the aforementioned parameters on the performance of the Doppler radar was observed, and the heart rate variability is calculated. In Ref. 3, a transceiver operating in the Ka band with low-power double-sideband signal transmission gave an accuracy above 80%. A detailed examination of the theoretical and realistic uses and limitations of the Doppler radar for heartbeat detection can be found in Ref. 4.

In 2002, the Federal Communication Commission (FCC) allowed the unlicensed use of ultra-wideband (UWB) from 3.1 to 10.6 GHz at low-power levels of −41.3 dBm/MHz [6]. The properties that make UWB useful for medical purposes include (i) high penetration power, (ii) low electromagnetic interference, (iii) low specific absorption rates, (iv) low power consumption, (v) small size, and (vi) low multipath interference leading to high reliability. The properties of UWB mentioned above are desired for accurate detection of heartbeat using Doppler radar, so the UWB range will be used here.

Wavelet Transform is utilized frequently in various signal-processing applications, because of its unique properties. It is specifically designed to work with nonstationary signals. It has been applied for data compression [7], image processing [8], ECG [9], and so forth.

In this letter, we propose to use wavelet transform for the first time to study and identify the heart rate from a phase-modulated Doppler radar signal. The wavelet transform is a fitting choice to analyze the heart rate signal as the heart rate signal is nonstationary and has sharp peaks. Using the time and frequency retention properties of wavelet transform, new coefficients were described and used to study the fine properties of the heart rate signal obtained from Doppler radar. Swift and slow changes in heart rate could be observed and comparison with a reference heart rate from an ECG device showed promising similarity giving an indication of the good accuracy. Vivaldi antennas provided excellent performance as the transmitting and receiving antenna for the Doppler radar. Section 2 deals with the theory behind Doppler radar cardiopulmonary monitoring. Section 3 details the experimental arrangement. In Sections 4 and 5, the results and the conclusions are discussed, respectively.

## 2. THEORY

The human chest has a quasi-periodic motion due to breathing (expansion and contraction of the lungs) and heart beating. A single tone continuous wavelet (CW) when reflected from the chest is phase modulated by this quasi-periodic motion according to Doppler theory. The returned signal is given by:

$$\Delta\theta = \frac{4\pi\Delta x(t)f}{c} \tag{1}$$

where $\Delta\theta$ is the phase variation, $\Delta x(t)$ is the chest motion, $c$ is the speed of light, and $f$ is the frequency of the CW. Equation 1 shows the directly proportional relationship of phase variation with the chest motion $\Delta x(t)$ and frequency $f$ of the CW. The average heartbeat rate is between 40 and 160 beats per minute (BPM), and the breathing rate average is between 12 and 18 breaths per minute. The received signal contains information about breathing rate and heartbeat rate. It also contains noise due to clutter, coupling of antennas, and the internal noise of the radar. The heartbeat signal is weak when compared with the

# ERRATUM: ANOMALOUS FORERUNNERS IN WAVE PROPAGATION INTERPRETED BY A TYPICAL DIFFRACTION INTEGRAL

**A. Ranfagni,[1] I. Cacciari,[1] R. Ruggeri,[2] A. Agresti,[3] R. Mignani,[4] A. M. Ricci,[5] and A. Petrucci[4]**
[1] Istituto di Fisica Applicata "Nello Carrara" del Consiglio Nazionale delle Ricerche, via Madonna del Piano 10, 50019 Sesto Fiorentino, Firenze, Italy
[2] Istituto dei Sistemi Complessi del Consiglio Nazionale delle Ricerche, Sezione di Firenze, via Madonna del Piano 10, 50019 Sesto Fiorentino, Firenze, Italy
[3] Dipartimento di Fisica dell'Universita' di Firenze, via G. Sansone 1, 50019 Sesto Fiorentino, Firenze, Italy
[4] Dipartimento di Fisica "Edoardo Amaldi" Universita' degli Studi di Roma "Roma Tre", via della Vasca Navale 84, 00146 Roma, Italy
[5] Istituto per le Telecomunicazioni e l'Elettronica della Marina Militare "Giancarlo Vallauri" (Mariteleradar), Viale Italia 72, 57100 Livorno, Italy

*Received 11 November 2010*

**ABSTRACT:** *Originally published Microwave Opt Technol Lett 53: 1789–1793, 2011* © 2011 Wiley Periodicals, Inc. Microwave Opt Technol Lett 53:2448, 2011; View this article online at wileyonlinelibrary.com. DOI 10.1002/mop.26369
(Original article DOI: 10.1002/mop.26133)

Please note the following corrections to this article:

In Section 1 the references a), b), c) and d) should be read [2], [3], [4], and [5], respectively.

In Eq. (4) of Section 2, the notation "Im b0" should be read Im $b \gtrless 0$.

The caption of Figure 1 should be read only up to $-iy$.

The following sentences starting from "coincident in the original integration path as well as in the SDP, the first integral in Eq. (3) diverges and $I(\Omega) \rightarrow \infty$. A third conclusion.... with Eq. (4), with b = 0. "In our cases, however, we never realize this situation.", should be added at the end of Section 2.

At the end of the penultimate paragraph of Section 2, the quantity "$\pi;i$ res$[f(z \rightarrow \beta)]$" should be read $\pi i$ res$[f(z \rightarrow \beta)]$.

In the caption of Table 1 substitute $\Omega I_f$ and $\Omega I_0$ with $I_f$ and $I_0$.

A few lines before the end of Section 3, substitute "the quantity $a$ could be $\gg 1$" with "the quantity $a$ could be $\ll 1$".

In Section 4, at the end of second paragraph, Ref. [20] should be read [22].

In the third paragraph of Section 4 the relation $I_f \infty |I(\Omega)|^2$ should be read $I_f \propto |I(\Omega)|^2$.

In the forth paragraph of Section 4 the word "integration-ath" should be read "integration-path".

After Eq. (8) in Section 4 the relation $\xi \lesssim 1$ should be read $\xi \gtrsim 1$.

Also after Eq. (8) the notation $a\Omega 1$ should be read $a \ll 1$.